

*Short Communication*

# **Porous Activated Carbon Prepared from Highland Barley Straw by Phosphoric Acid Activation as a Conductive Agent for Improving Electrochemical Performance of LiFePO<sub>4</sub> Cathodes**

Wenliang Sun\*, Rusi Hao

College of Chemical Engineering, Qinghai University, Xining 810016, China

\*E-mail: [sunwl3@hotmail.com](mailto:sunwl3@hotmail.com)

*Received:* 20 November 2020 / *Accepted:* 23 January 2021 / *Published:* 28 February 2021

---

Herein, porous activated carbon was synthesized from highland barley straw by phosphoric acid activation and used as a conductive agent for LiFePO<sub>4</sub> cathodes. The morphology and microstructure are characterized by scanning electron microscopy and nitrogen adsorption and desorption. The results show that the porous activated carbon convenient three-dimensional porous microstructure. Compared with the conventional conductive agent carbon black Super P, the obtained porous activated carbon presents a high capacity of 153.63 mA h g<sup>-1</sup> at 0.1 C, as well as an excellent rate performance and cycling stability. The simple method for the preparation of porous activated carbon as a conductive agent with an excellent electrochemical performance opens up a new opportunity of LiFePO<sub>4</sub> cathodes for widespread applications in lithium-ion batteries.

---

**Keywords:** LiFePO<sub>4</sub> cathode; Conductive agent; Biomass; Activated carbon; Highland barley straw

## **1. INTRODUCTION**

In the recent years, because of the advantages include large theoretical specific capacity, long cycle life, high thermal stability, low cost, safety characteristic and environment compatibility, Lithium iron phosphate (LiFePO<sub>4</sub>) has been widely used as the cathode materials in lithium-ion batteries especially in electric vehicles (EVs) [1]. However, sluggish kinetics of electron and lithium-ion conductivities limit the commercial application of LiFePO<sub>4</sub> batteries [2]. A number of methods such as doping with exotic ions, reducing the LiFePO<sub>4</sub> particle size, controlling the morphology and coating carbon on LFP have been used to optimize the limitation of electronic and ionic transportations for improving the electrochemical performance of LiFePO<sub>4</sub> [3-6]. Furthermore, with the emergence of a variety of new functional carbon materials, various advanced carbon materials such as graphene, carbon nanotube and mesoporous carbon materials have been widely applied as a conductive agent with

LiFePO<sub>4</sub> to improve the electron and ion transportation [7-8]. Compared to traditional carbon coating materials, the introduction of advanced functional carbon materials provides a better way to improve the performance of LiFePO<sub>4</sub> (named LFP) because of the superior specific surface area, good structural stability and excellent conductive performance [9-10].

As a porous carbon material, activated carbon has been widely studied in the fields of energy storage devices, such as lithium-ion batteries and supercapacitors, due to its excellent electrochemical properties, high specific surface area, excellent chemical stability, low price and simple preparation process [11-12]. Many studies have been reported that activated carbon can be prepared from various renewable and abundant carbon sources and various natural biomass-derived carbon materials have been applied for the preparation of porous activated carbon as electrode materials because of their advantages in low toxicity, cheap, readily available, renewable, etc [13-14].

It is common to use the addition of conductive additive into the LiFePO<sub>4</sub> cathodes to improve electrochemical performance. Among the various of conductive materials, carbon conductive agents are the most widely used materials in LiFePO<sub>4</sub> cathodes. Li et al. combined with mechanical mixing and annealing method for the preparation of reduced graphene oxide and Mg<sup>2+</sup> to LiFePO<sub>4</sub> composite to largely improved electrochemical performance of the cathode [15]. Piao et al. developed a novel prepared the cellulose nanofiber derived carbon and reduced graphene oxide co-supported LiFePO<sub>4</sub> nanocomposite, which exhibits good rate performance (discharge capacity of 168.9 mA h g<sup>-1</sup> at 0.1C, and 90.3 mA h g<sup>-1</sup> at 60 C) [16]. Shi et al. synthesized the LiFePO<sub>4</sub>/C composite with unique copolymer carbon resource PAN-b-PMMA via in situ carbothermal reduction method. This composite cathode shows rate capability (165.3 mA h g<sup>-1</sup> at 0.2 C vs. 78.9 mA h g<sup>-1</sup> at 30 C) and cycle stability (98% cycle retention after 100 cycles at 0.2 C) [17]. All these methods mentioned above require rigorous procedures, long time and high cost. It is necessary to develop conductive agents for LiFePO<sub>4</sub> cathode with excellent electrical conductivity, low cost and environmental benignity.

Highland barley straw is a typical crops biomass waste in high altitude areas and it should be recycled for the ecological environment protection and sustainable development. In this work, we use highland barley straw as a biomass carbon precursor for the preparation of the porous activated carbon by using chemical activation method through direct pyrolysis of the precursor impregnated with activating agent H<sub>3</sub>PO<sub>4</sub> [18]. The as-prepared porous activated carbon were used as a conductive agent to improve the electrochemical properties of LiFePO<sub>4</sub> (named LFP) cathode materials. Compared with the usual carbon black, the as-prepared porous activated carbon shows excellent properties that the capacity, rate and cycling performance of LFP cathodes can be enhanced as the conductive agent. The reason may be that the biomass-based porous activated carbon provides an efficient, convenient three-dimensional structure for better contact with LFP so that the lithium ion can pass through smoothly during the lithiation/delithiation process. This approach provides a potential application for biomass in improving the electrochemical performance of LFP.

## 2. EXPERIMENTAL

### 2.1. Materials and reagents

The commercial available  $\text{LiFePO}_4$  powders (with about 2 wt% carbon) were from Tianjin STL Energy Technology Co., Ltd., China. Phosphoric acid  $\text{H}_3\text{PO}_4$  (>85 wt% in  $\text{H}_2\text{O}$ ) was obtained from Aladdin (Shanghai, China). All of the other chemicals were of analytical grade and used without further purification. The water used throughout the experiment was purified by Milli-Q (>18 M $\Omega$ /cm).

### 2.2. Material synthesis

Highland barley straw was collected from the farms located in the campus of Qinghai University. After washing with deionized water, the straw was directly dried in vacuum at 80 °C overnight until its quantity was constant. The sample was cut into fractions and then immersed with 85 wt%  $\text{H}_3\text{PO}_4$  in an impregnation ratio of 1:4 for 10 h. The as-obtained mixture was pre-activated in an oven at 140 °C for 1.5 h. After that, the sample was carbonized under  $\text{N}_2$  flow (150 mL  $\text{min}^{-1}$ ) with a heating rate of 10 °C  $\text{min}^{-1}$ , until the final temperature of 600 °C for 1.5 h. The porous activated carbon was allowed to cool down to room temperature under the continuous flow of  $\text{N}_2$ . The sample was washed with 0.1 M hydrochloric acid solution and deionized water to remove the unreacted impurity content. Thereafter, the mixture was heated several times and brought to boiling for 1 min until neutral pH. Finally, the prepared porous activated carbon was dried at 120 °C for 8 h in vacuum at 80 °C overnight to get the products.

### 2.3. Material Characterizations

The morphology of porous activated carbon was examined JSM-6610 scanning electron microscopy (SEM, JEOL, Japan). Brunauer-Emmett-Teller (BET) measurements were carried out using an 3H-2000PS4 specific surface & pore size analyzer (BeiShiDe, China).

### 2.4. Electrochemical measurements

For cathode electrodes preparation, the electrode of LFP with the obtained porous activated carbon as a conductive agent (denoted as LFP-AC) was firstly prepared by mixing active material LFP (80% wt%), the synthesized porous activated carbon (10% wt%) and polyvinylidene difluoride (PVDF, 10% wt%) in N-methyl-2-pyrrolidone (NMP) and all were mixed until thoroughly combined. Then the formed slurry was laminated on aluminum foil as a current collector with about 0.2 mm in thickness, dried under an air atmosphere at 60 °C for 2 h and a vacuum atmosphere at 110 °C for 8 h to remove NMP. The electrode was cut into disks of 15.5 mm in diameter and pressed by a calender to a predetermined area density (ca. 8 mg  $\text{cm}^{-2}$ ). The electrode of LFP with conventional carbon black as conductive agent was prepared by using carbon black (Super P) as a conductive agent in the slurry (denoted as LFP-SP) via the same procedure as above.

The electrochemical performances for the LFP cathodes were characterized by using CR2032 coin-type cells (20 mm diameter and 3.2-mm thick). Lithium metal was used as the anode electrode; microporous polypropylene membrane (Celgard 2325) served as the separator; the nonaqueous electrolyte was 1 M  $\text{LiPF}_6$  in a 1:1 solvent mixture of ethylene carbonate (EC)/dimethyl carbonate (DMC). The cells were assembled in a glove box with a high purity argon atmosphere and tested at room temperature. Galvanostatic charging-discharging, cycling and rate capability tests were conducted by battery testing system (CT2001A, LAND Co., China) at different current densities ( $1 \text{ C} = 170 \text{ mA h g}^{-1}$ ) within the voltage range of 2.2–4.2 V. The cyclic voltammetry (CV) measurements were performed with a PGSTAT204 electrochemical workstation (Metrohm-Autolab) in the range of 2.0–4.8 V at 0.2 mV by a PGSTAT204 electrochemical workstation with the frequency ranging from 0.01 Hz to 100 kHz and a AC signal of 5 mV in amplitude as the perturbation.

### 3. RESULTS AND DISCUSSION

#### 3.1. Preparation and characterization of porous activated carbon

The fabrication of porous activated carbon (AC) derived from highland barley straw as a conductive agent for  $\text{LiFePO}_4$  cathodes is schematically depicted in Fig. 1.

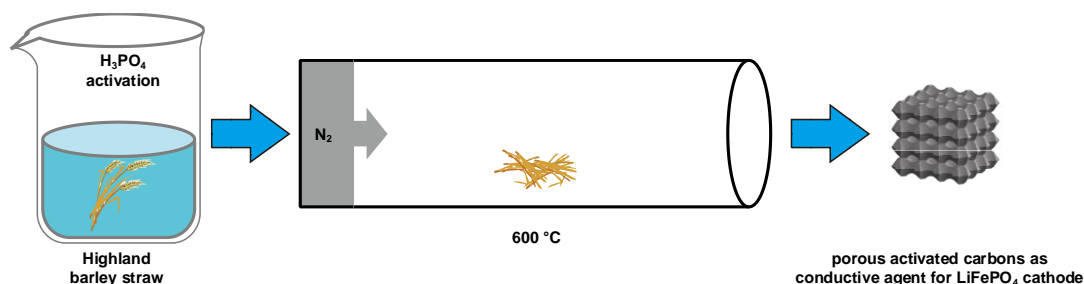


**Figure 1.** Schematics of the porous activated carbon prepared from highland barley straw by phosphoric acid activation for use as a conductive agent for  $\text{LiFePO}_4$  cathode materials

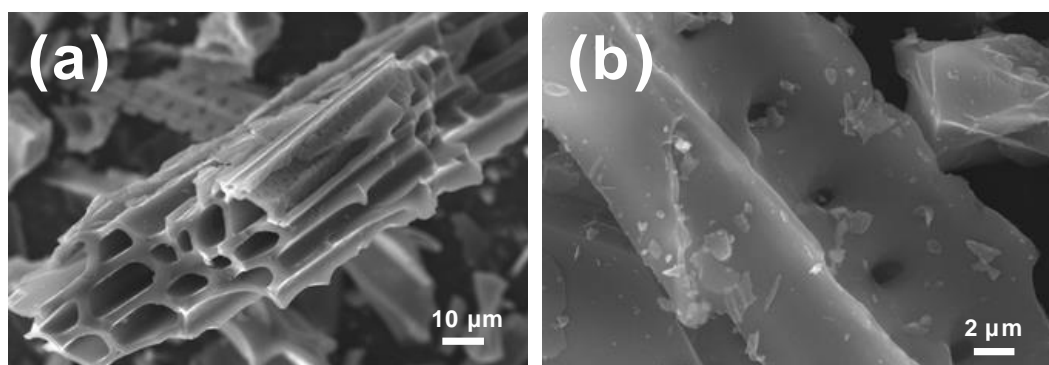


**Figure 2.** (a, b) SEM images of the porous activated carbon prepared from highland barley straw.

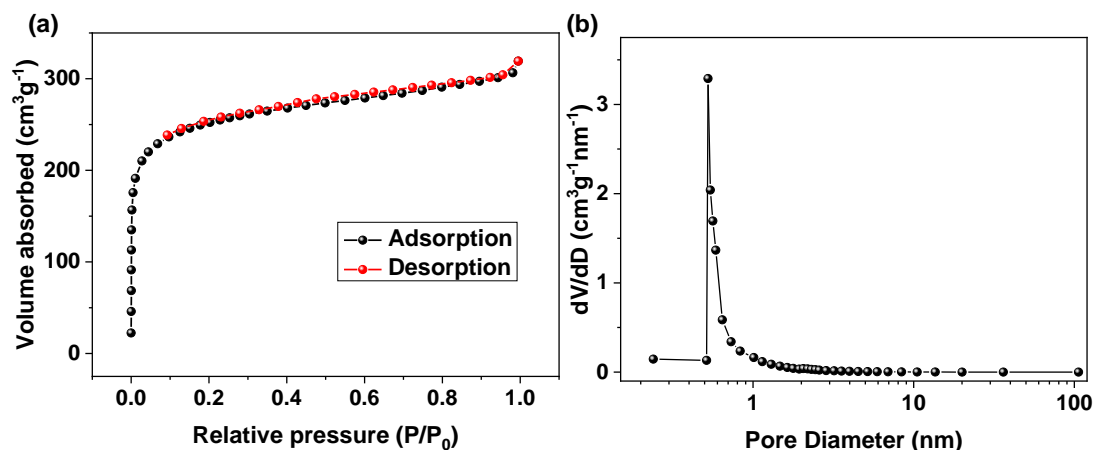


**Figure 3.** (a) Nitrogen adsorption and desorption isotherms of the porous activated carbon, (b) pore size distribution curves of the porous activated carbon.

To create rich porous structure, the  $\text{H}_3\text{PO}_4$  was employed as activation agents to obtain large surface area porous activated carbon. Fig. 2 shows a typical SEM images of the porous activated carbon. The activated carbon is composed of distinct crumpled carbon sheets with a large number of pores. Fig. 3a and b exhibit  $\text{N}_2$  sorption isothermals and corresponding curves of pore size distribution, which indicate the porosity of AC. According to the classification of the International Union of Pure and Applied Chemistry, AC is found to be type I isotherm curve with the steep increase at a relative pressure  $P/P_0 < 0.05$ , which means abundant micropores in carbon materials [19]. The activated carbon has a large surface area of  $931.23 \text{ m}^2 \text{ g}^{-1}$  and a total pore volume of  $0.344 \text{ cm}^3 \text{ g}^{-1}$ . The average pore diameter is 2.5 nm, calculated from the desorption branch of the nitrogen isotherm with the BJH method. The rapid rise of the barley straw and activating agent  $\text{H}_3\text{PO}_4$  to high temperature makes their mixing more complete and further makes the reaction more intense. Phosphoric acid has a dissolution and erosion effect on raw biomass at high temperature, and acts as the skeleton of carbon through vaporization and impregnation, which also increases the formation of micropores. Besides, The pore size of AC samples is mostly distributed within 2.5 nm. It can be seen that the pore size of the samples is mainly concentrated within the range of micropores, thus forming a large specific surface area and expanding the tunnel for lithium ion diffusion. The special microporous structure can absorb and maintain more electrolyte, accelerate the diffusion rate of lithium ion, and enhance the lithium ion conductivity of electrode.

### 3.2 Electrochemical performance characterizations

The electrochemical properties of the LFP cathodes with the synthesized porous activated carbon (LFP-AC) and the conventional carbon black Super P (LFP-SP) as a conductive agent were evaluated.

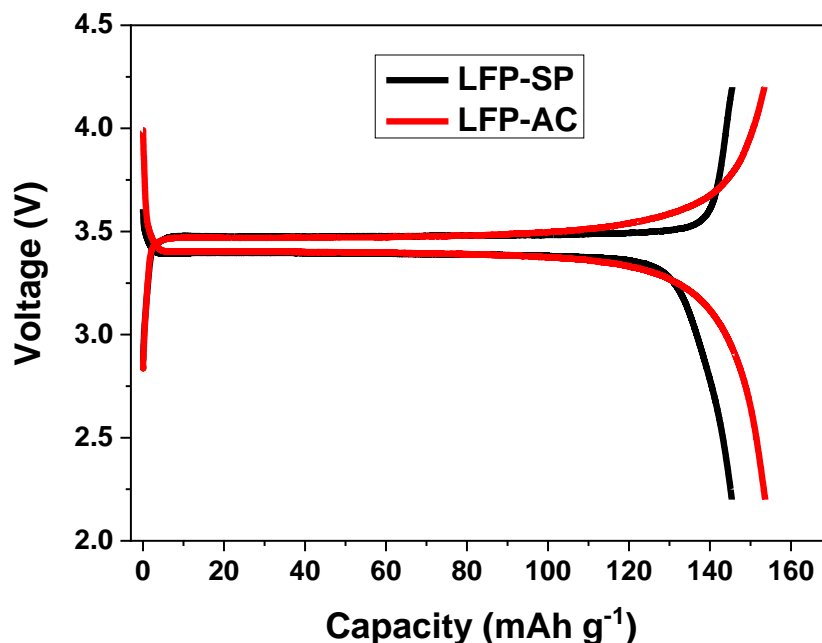


**Figure 4.** The voltage profiles for the first cycle charging and discharging (with a rate of 0.1 C) of the LFP-AC and LFP-SP cathodes in a voltage range of 2.2–4.2 V..

Fig. 4 shows the that the galvanostatic charge-discharge curves of the first cycle with 0.1 C as the charging and discharging rate between 2.2 and 4.2 V for the cathodes with the synthesized porous activated carbon (AC) as a conductive agent percentages become different from that with the conventional Super P (SP). Typical flat voltage plateau at about 3.4 V (vs.  $\text{Li}^+/\text{Li}$ ) can be observed, corresponding to the  $\text{Fe}^{3+}/\text{Fe}^{2+}$  redox process together with  $\text{Li}^+$  extraction/insertion for both of the electrodes [20]. The LFP-AC cathode delivered a discharge capacity of  $153.63 \text{ mA h g}^{-1}$  at a low discharge rate of 0.1 C, which is higher than the capacity of the conventional LFP-SP cathode ( $145.38 \text{ mA h g}^{-1}$ ). This improved discharge capacity can be attributed that the Li ion in the LFP-AC cathode can migrate more quickly along the special microporous structure framework.

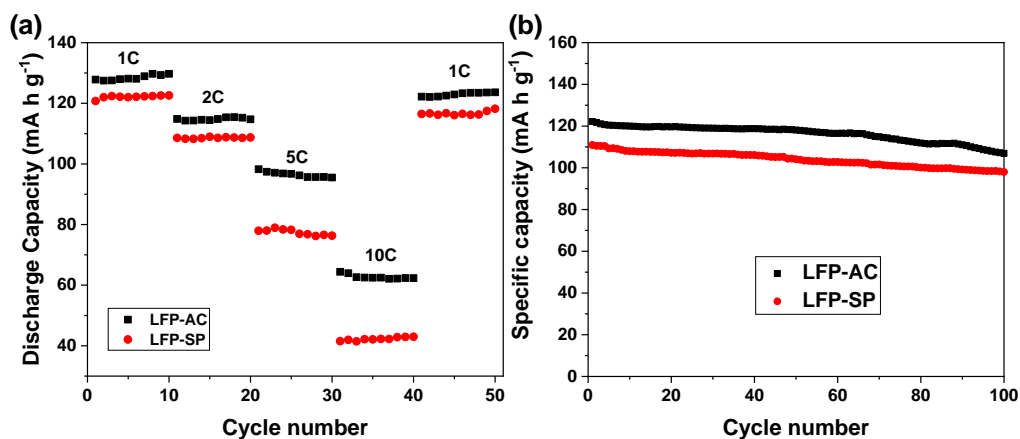


**Figure 5.** (a) Discharge capacities at various rates of LFP-AC and LFP-SP electrodes, (b) cycling stability of LFP-AC and LFP-SP electrodes at a rate of 2C.

Fig. 5a shows the rate capabilities of the LFP-AC and LFP-SP at different current density. Both of the electrodes were cycled at various charge/discharge rates ranging from 1 to 10 C and then reversed back to low current density at 1 C. Very similar rate performance is observed for LFP-AC and LFP-SP electrodes at discharge rates from 1 C to 2 C. However, the special capacity of LFP-AC respectively reach 98 and 64 mA h g<sup>-1</sup> at high rates of 5 C and 10 C, which is much better than those of LFP-SP electrode.

**Table 1.** Comparison of the electrochemical performance of the LiFePO<sub>4</sub> cathode with the carbon-relative conductive additive in the recent published literatures.

Composite	Preparation method	Rate performance, mA h g <sup>-1</sup> (rate, C)	Cycling performance	References
LFP <sup>a</sup> /graphene	Physical mixing	112.4 (30 C), 96.7 (50 C)	3.7 % capacity fading at 30 C after 300 cycles	[21]
LFP/graphene aerogel	Hydrothermal reaction	167 (0.1 C), 120 (10 C)	11.5 % capacity fading at 1 C after 800 cycles	[22]
LFP/carbon nanofiber	One-pot electrospinning method	152 (0.5 C)	<1.8 % capacity fading at 30 C after 300 cycles	[23]
LFP/carbon nanotube	Solid-station reaction	123 (10 C)	<1.6 % capacity fading at 10 C after 1000 cycles	[24]
LFP/carbonized acetylenic carbon-rich polymer	Solid-station reaction	129.6 (50 C)	No obvious fading at 20 C after 100 cycles	[25]
LFP/ graphene oxide-silver joint conductive agent	Physical mixing	150 (0.5 C)	No obvious fading at 0.1 C after 30 cycles	[26]
LFP/porous activated carbon	Solid-station reaction	153 (0.1 C), 98 (5 C)	2 % capacity fading at 2 C after 100 cycles	this work

<sup>a</sup> LiFePO<sub>4</sub>

Good cycle life performances of both the LFP-SP and LFP-AC samples (tested at a rate of 2 C) are observed shown in Fig. 5b. The cyclability of LFP-AC cathode material have no significant capacity loss after 100 cycles at high current density (170 mA h g<sup>-1</sup>, 2 C); the capacity retention of LFP-AC over 100 cycles remains 98%, which is similar with LFP-SP. The result clearly indicate that the as-prepared porous activated carbon as the conductive agent exhibits excellent cyclability with no obvious capacity loss in 100 cycles. Furthermore, we compared our results with some published reports which summarized in Tab. 1 about the electrochemical performance of the LiFePO<sub>4</sub> cathode with the carbon-relative conductive additive. It can be seen that the present porous activated carbon as a conductive agent show the same excellent rate and cycling performance as these reported literatures. Meanwhile, it has been shown that the preparation process in this work is facile and eco-friendly and it provide a simple and effective way for the conductive additive of LiFePO<sub>4</sub> cathode.

Fig. 6a presents the cyclic voltammogram (CV) performances of LFP-AC and LFP-SP at a scan rate of 0.2 mV s<sup>-1</sup>. The symmetry of the sharp oxidation and reduction peaks in the CV curves confirms the good reversibility of lithium extraction/insertion reactions. The LFP-AC exhibits a higher peak current than that of LFP-SP cathode, indicating a better rate capability. Furthermore, the potential difference between anode and cathode peaks for LFP-AC and LFP-SP is respectively 0.544 V and 0.471

V. The smaller potential difference for the porous activated carbon as the conductive agent implies better electrochemical reversibility of electrode reaction due to the efficient conductive framework.

The electrochemical impedance spectra (EIS) of LFP-AC and LFP-SP are shown in Fig. 6b. appropriate equivalent circuit model (inset in Fig. 6b) is constructed to fit the impedance spectra.

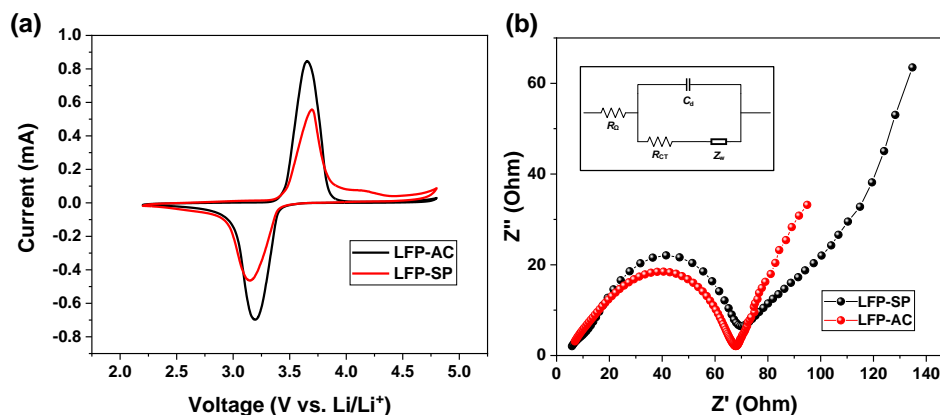


**Figure 6.** (a) Cyclic voltammograms of LFP-AC and LFP-SP at a scan rate of  $0.2 \text{ mV s}^{-1}$ , (b) electrochemical impedance spectra of LFP-AC and LFP-SP electrodes in the frequency range of 100 kHz to 10 mHz. Inset: Equivalent circuit.

An intercept at the real resistance axis in high frequency corresponded to the ohmic resistance ( $R_{\Omega}$ ), which represented the resistance of the electrolyte. The semicircle in the middle frequency range indicated the charge transfer resistance ( $R_{ct}$ ). The straight line in the low frequency region represented the Warburg impedance ( $Z_w$ ), which was associated with lithium-ion diffusion in the  $\text{LiFePO}_4$  particles [27]. The diameter of the semicircle on the real axis can be approximately equal to  $R_{ct}$ . The charge transfer resistance can be attributed to the electrochemical reaction at the cathode–electrolyte interface. It can be seen that the  $R_{ct}$  value for LFP-AC cathode is about  $67 \Omega$ , similar with that of LFP-SP ( $70 \Omega$ ). The results demonstrate that the electronic conductivity of the porous activated carbon prepared from highland barley straw can be appropriate as the conductive agent for the  $\text{LiFePO}_4$  cathode materials.

#### 4. CONCLUSIONS

The porous activated carbon was successfully synthesized from highland barley straw with suitable electrical conductivity, high specific surface area and ordered structure. Compared with the conventional conductive agent carbon black Super P, the porous activated carbos as the conductive agent for the  $\text{LiFePO}_4$  cathode exhibit the excellent electrochemical performance with a high reversible capacity and good rate performance, which allow better irrigation of electrolyte and provide a large electrochemical surface for enhancing the lithium ion conductivity of electrode. Therefore, The porous activated carbon prepared from highland barley straw has great potential in conductive agent applications for improving their electrochemical properties.

## ACKNOWLEDGMENTS

We gratefully acknowledge the financial support from the National Natural Science Foundation of China (NSFC Grants No. 21865024), the Natural Science Foundation of Qinghai Province, China (Grants No. 2017-ZJ-946Q), the Science Foundation for The Youth Scholars of Qinghai University (Grants No. 2019-QGY-6) and Thousand Talents Program of Qinghai Province.

## References

1. J. Wang, and X. Sun, *Energy Environ. Sci.*, 8 (2015) 1110.
2. Y. Wang, P. He, and H. Zhou, *Energy Environ. Sci.*, 4 (2011) 805.
3. S. M. Oh, S. T. Myung, J. B. Park, B. Scrosati, K. Amine, and Y. K. Sun, *Angew. Chem. Int. Ed.*, 51 (2012) 1853.
4. E. Meng, M. Zhang, Y. Hu, F. Gong, L. Zhang, and F. Li, *Electrochim. Acta*, 265 (2018) 160.
5. A. Eftekhari, *J. Power Sources*, 343 (2017) 395.
6. J. Ni, Y. Zhao, J. Chen, L. Gao, and L. Lu, *Electrochem. Commun.*, 44 (2014) 4.
7. X. Wei, Y. Guan, X. Zheng, Q. Zhu, J. Shen, N. Qiao, S. Zhou, and B. Xu, *Appl. Surf. Sci.*, 440 (2018) 748.
8. B. Lung-Hao Hu, F.-Y. Wu, C.-T. Lin, A. N. Khlobystov, and L.-J. Li, *Nat. Commun.*, 4 (2013) 1687.
9. C. Gong, Z. Xue, S. Wen, Y. Ye, and X. Xie, *J. Power Sources*, 318 (2016) 93.
10. Y. Wang, Y. Wang, E. Hosono, K. Wang, and H. Zhou, *Angew. Chem. Int. Ed.*, 47 (2008) 7461.
11. Y. Guan, J. Shen, X. Wei, Q. Zhu, X. Zheng, S. Zhou, and B. Xu, *Electrochim. Acta*, 294 (2019) 148.
12. N. Böckenfeld, T. Placke, M. Winter, S. Passerini, and A. Balducci, *Electrochim. Acta*, 76 (2012) 130.
13. Y. Guo, C. Tan, J. Sun, W. Li, J. Zhang, and C. Zhao, *Chem. Eng. J.*, 381 (2020) 122736.
14. Y. Liu, Z. An, M. Wu, A. Yuan, H. Zhao, J. Zhang, and J. Xu, *Chin. Chem. Lett.*, 31 (2020) 1644.
15. Y. Huang, H. Liu, L. Gong, Y. Hou, and Q. Li, *J. Power Sources*, 347 (2017) 29.
16. S. Park, J. Oh, J. M. Kim, V. Guccini, T. Hwang, Y. Jeon, G. Salazar-Alvarez, and Y. Piao, *Electrochim. Acta*, 354 (2020) 136707.
17. M. Shi, R. Li, and Y. Liu, *J. Alloy. Compd.*, 854 (2021) 157162.
18. Q. Han, J. Wang, B. A. Goodman, J. Xie, and Z. Liu, *Powder Technol.*, 366 (2020) 239.
19. M. Liu, J. Qian, Y. Zhao, D. Zhu, L. Gan, and L. Chen, *J. Mater. Chem. A*, 3 (2015) 11517.
20. Y. Liu, J. Gu, J. Zhang, F. Yu, J. Wang, N. Nie, and W. Li, *RSC Adv.*, 5 (2015) 9745.
21. Y. Guan, J. Shen, X. Wei, Q. Zhu, X. Zheng, S. Zhou, and B. Xu, *Appl. Surf. Sci.*, 481 (2019) 1459.
22. X. Tian, Y. Zhou, X. Tu, Z. Zhang, and G. Du, *J. Power Sources*, 340 (2017) 40.
23. Z. Cao, M. Sang, S. Chen, J. Jia, M. Yang, H. Zhang, X. Li, and S. Yang, *Electrochim. Acta*, 333 (2020) 135538.
24. Y. Q. Qiao, W. L. Feng, J. Li, and T. D. Shen, *Electrochim. Acta*, 232 (2017) 323.
25. Y. Mo, J. Liu, C. Meng, M. Xiao, S. Ren, L. Sun, S. Wang, and Y. Meng, *Carbon*, 147 (2019) 19.
26. P. R. Ilango, R. Gnanamuthu, Y. N. Jo, and C. W. Lee, *J. Ind. Eng. Chem.*, 36 (2016) 121.
27. R. Chen, Y. Wu, and X. Y. Kong, *J. Power Sources*, 258 (2014) 246.